NASA CONTRACTOR REPORT

NASA CR-1490

NASA CR-149

c. 1

VIBRATION CHARACTERISTICS OF A CYLINDER PARTIALLY FILLED WITH LIQUID WITH AN ATTACHED ELASTIC DRAIN PIPE

by Robert J. Kroll and Gerard G. Ventre

NATIONAL AERONAUTICS AND SPACE ADMINISTRATION • WASHINGTON, D. C. • JANUARY 1970

VIBRATION CHARACTERISTICS OF A CYLINDER

PARTIALLY FILLED WITH LIQUID WITH

AN ATTACHED ELASTIC DRAIN PIPE

By Robert J. Kroll and Gerard G. Ventre

ABSTRACT

The unforced frequencies and mode shapes for the longitudinal vibrations of an elastic-fluid-gas system are determined. This system simulates a fuel tank and drain pipe subsystem of a liquid fueled launch vehicle including the effects of the liquid and ullage gas.

A Rayleigh-Lagrange solution was developed and a computer program was written for the analysis of the system having any dimensions and physical properties. Frequencies and mode shapes can be found for all liquid heights. Thus, the effect of fuel consumption can be simulated.

Axisymmetric breathing of the structure and the flexibility of the tank bottom were found to strongly influence the system response. However, the ullage gas had only a small effect and asymmetric breathing had no effect on the longitudinal system response.

Good correlation was obtained between experimental frequencies determined at NASA Langley Research Center on several system configurations and those calculated by the method developed herein.

Parametric studies were conducted to determine families of systems that have the same frequencies at varying liquid levels.

TABLE OF CONTENTS

LIST OF FIGURES

VIBRATION CHARACTERISTICS OF A CYLINDER PARTIALLY FILLED
WITH LIQUID WITH AN ATTACHED ELASTIC DRAIN PIPE

BY

Robert J. Kroll and Gerard G. Ventre
University of Cincinnati

INTRODUCTION

Statement of the Problem

The longitudinal vibrations of an elastic-fluid-gas system are investigated. This system, chosen to simulate a fuel (or oxidizer) tank and drain pipe subsystem of a liquid fueled launch vehicle, consists of an elastic structure partially filled with a liquid and pressurized with an ullage gas above the liquid. As the quantity of liquid in the system decreases, corresponding to fuel consumption, the frequencies and mode shapes change.

The main purpose of this investigation is to determine the influence of the variable liquid mass on the free longitudinal frequencies and mode shapes of the system. The relative importance of the system parameters are also studied.

Background

Flexural vibrations of a launch vehicle are important because of their effect on its control sensors. However, longitudinal vibrations were considered to be unimportant until the advent of manned launch vehicles. During their peak amplitude these longitudinal vibrations, called "POGO" oscillations, can temporarily affect the performance of a man.

Many authors have investigated different aspects of the POGO oscillations, which occur primarily in liquid fueled launch vehicles. The complete POGO problem involves interaction among the structure, the liquid, the ullage gas, and the variations in thrust. Bauer (refs. 1,2,3), Hutton (ref. 4), Bhuta and Koval (ref. 5), and Tong (ref. 6) considered structure-fluid interactions with primary emphasis on fluid motion. Fung et al. (ref. 7) considered the effect of an internal gas on the vibration of shells. Mixson and Herr (ref. 8), Leroy (ref. 9), Chu (ref. 10), and Chu and Kana (ref. 11) treated the breathing vibration of shells containing a liquid. Uchiyama and Tai (ref. 12) considered

longitudinal vibrations of a tank containing a liquid. Runyan et al. (ref. 13) analyzed the longitudinal vibrations of shells with liquid and ullage gas, using a lumped parameter analysis. Pinson et al. (ref. 14) investigated the longitudinal vibrations of an entire launch vehicle, using a lumped parameter analysis, with the added provision of accounting for shell radial motion. Pengelley (ref. 15) considered longitudinal vibrations of cone-cylinder combination shells including the effect of an imcompressible liquid and a compressible ullage gas, but neglecting sloshing and the kinetic energy of the radial motion of the liquid.

In this investigation a continuous analysis of the system described above is performed. All of the following effects are included: (1) sloshing of the liquid, (2) radial and longitudinal kinetic energy of the liquid, (3) compressibility of the ullage gas, (4) flexibility of the structure in both the longitudinal and radial directions, and (5) the influence of breathing on the longitudinal vibrations. As previously mentioned, this is an analysis of a subsystem of an entire launch vehicle.

Technical Approach

A Rayleigh-Lagrange analysis is used. Structural displacement functions containing arbitrary coefficients are assumed. These arbitrary coefficients are the generalized displacement coordinates. Next the motion of the liquid is made compatible with the structural displacements. A compressible ullage gas, which is contained in the closed volume above the liquid, is compressed and expanded as the liquid rises and falls and acoustic waves travel through the gas. The potential and kinetic energies of the structure, liquid, and gas are substituted into Lagrange's equation, which yields the general characteristic value solution for the frequencies and mode shapes.

A computer program, in which any geometry and properties of the system can be input, is developed to calculate the frequencies and mode shapes at all liquid levels. Using this program, extensive parametric studies are made to determine the importance of all system variables and the effects of breathing, ullage gas, structural flexibility, and the configuration of the drain pipe.

LIST OF SYMBOLS

Symbol	Definition
$[A]$	Stiffness matrix
$A_{si}(t)$	Integration parameter in equation (11) on page 10
a	Radius of pipe
a'	a/R
B	Adiabatic bulk modulus of elasticity of gas
$[B]$	Mass matrix
$B_{si}(t)$	Integration parameter in equation (11) on page 10
c	Speed of sound in gas
D	$\dfrac{Eh^3}{12(1-\mu^2)}$
$D_{sj}(t)$	Integration parameter in equation (11) on page 10
E	Modulus of elasticity
$E_{sj}(t)$	Integration parameter in equation (11) on page 10
$G_s(t)$	Integration parameter in equation (11) on page 10
g	Acceleration due to gravity
g_1	See appendix A
H	Liquid height in tank
H'	H/R
H''	H/a
$H_s(t)$	Integration parameter in equation (11) on page 10
h	Thickness
$h_1, \ldots, h_7$	See appendix A
I_s	Modified Bessel function of first kind, order s
J_s	Bessel function of first kind, order s
K	$\dfrac{Eh}{1-\mu^2}$
k	Stiffness

3

k_{rj} Roots of $J_r' = 0$

L   Length of tank

L'   L/R

ℓ Length of pipe

ℓ' ℓ/a

$N(\eta, t)$ Function of η and t in equation (10) on page 9

n   Direction normal to surface

p   Pressure

$Q_n(t)$ Generalized displacement coordinate

q_i Generalized displacement coordinate in the i-direction

$\dot{q}_i$ Generalized velocity in the i-direction

R   Radius of tank

r   Radial coordinate

S   Surface area

T   Kinetic energy

t   Time

$U_n(t)$ Generalized displacement coordinate

u   Axial component of displacement

$u_n(t)$ Generalized displacement coordinate

$\overline{U}_n(t)$ Generalized displacement coordinate

V   Potential energy

$V_{rn}(t)$ Generalized displacement coordinate

Vol   Volume

v   Tangential component of displacement

W_{rn} Generalized displacement coordinate

w   Radial component of displacement

$w_n(t)$ Generalized displacement coordinate

$X(\xi, t)$ Function of ξ and t in equation (10) on page 9

z_1 See appendix A

z   Axial coordinate

Greek

α_p	$\omega^2 a/g$
α_t	$\omega^2 R/g$
Γ_n	$\dfrac{n\pi R}{L}$
γ	Ratio of specific heats
γ_n	$\dfrac{n\pi a}{\ell}$
$\gamma_{z\theta}$	Shear strain
Δ_n	$\dfrac{(2n-1)\pi}{2}$
δ	Dilatation
ε	Non-dimensional axial coordinate for pipe, $(Z-L)/a$
ε_z	Normal strain in z-direction
ε_θ	Normal strain in θ-direction
η	Non-dimensional radial coordinate for tank, r/R
$\Theta(\theta,t)$	Function of θ and t in equation (10) on page 9
Θ	Polar angle
Λ_n	$\dfrac{(2n-1)\pi R}{2L}$
λ_n	$\dfrac{(2n-1)\pi a}{2\ell}$
μ	Poisson's ratio
ξ	Non-dimensional axial coordinate for tank, z/R
ρ	Mass density
σ	Non-dimensional radial coordinate for pipe, r/a
ϕ	Velocity potential function
ω	Natural frequency

Subscripts

g	Gas
g_o	Gas at static equilibrium condition
ℓ	Liquid
o	Static equilibrium condition
p	Pipe

pb	Pipe bottom
t	Tank
tb	Tank bottom

Operators

∇	Del operator
$(\dot{\ })$	$d(\ )/dt$

Indices

i,j,k,m,n,p,r,s

ANALYSIS OF THE CONTINUOUS SYSTEM

Configuration of the System

The system used in this analysis is shown in Figure 1.

The upper cylinder represents a fuel or oxidizer tank. For this investigation the tank bottom is a flat plate. The lower cylinder represents the drain pipe.

A liquid, simulating the fuel or oxidizer, partially fills the tank and an ullage gas under pressure fills the tank above the liquid.

The top of the tank and the bottom of the drain pipe are closed with idealized rigid plates.

Assumptions

The entire system is supported from the top of the tank, which is stationary.

Figure 1.
System Configuration

The assumed structural displacements may be longitudinal, circumferential, and radial with the following constraints: (1) the top and bottom of the tank and pipe are simply supported, (2) the plate is simply supported at its outer radius, and (3) only axisymmetric bending of the plate is considered. Normally the tank and pipe are thin walled and have negligible discontinuity stresses, which is consistent with constraints (1) and (2). Small displacements are assumed and linear structural theory is used.

The liquid is incompressible and inviscid. Sloshing of the liquid is allowed at its free surface, but contact must be maintained at all structure-liquid interfaces. Draining of the liquid is considered to be quasistatic, thereby eliminating inertia effects associated with draining.
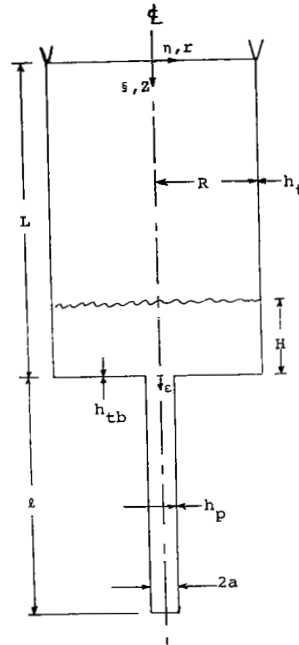
The ullage gas is ideal and compressible. Since the change of the liquid and gas volume due to draining is assumed to be quasistatic, the static ullage gas pressure is assumed constant at any liquid height. However, at a given liquid height there are dynamic gas pressure fluctuations, because the vibratory displacements change the gas volume. Longitudinal pressure waves in the ullage gas are considered, using a one dimensional equation which neglects the effect of radial motion of the tank walls on the gas. These pressure waves are totally reflected back into the gas at the top of the tank and at the liquid surface, because of the large acoustic impedance mismatch at these interfaces.

Kinematics of the Structure

The following structural displacements, which satisfy continuity requirements and are consistent with the assumptions listed above, are prescribed.

For the tank:

$$u_t = \sum_{n=1}^{\infty} U_n(t) \sin(\Lambda_n \S) \tag{1}$$

$$v_t = \sum_{r=1}^{\infty} \sum_{n=1}^{\infty} V_{rn}(t) \sin(\Gamma_n \S) \sin(r\theta) \tag{2}$$

$$w_t = \sum_{r=0}^{\infty} \sum_{n=1}^{\infty} W_{rn}(t) \sin(\Gamma_n \S) \cos(r\theta) \tag{3}$$

For the tank bottom:

$$u_{tb} = \sum_{n=1}^{\infty} U_n(t) \sin(\Lambda_n L') + \overline{U}_n(t) \cos(\Delta_n \eta) \tag{4}$$

For the pipe:

$$u_p = \sum_{n=1}^{\infty} \left[U_n(t) \sin(\Lambda_n L') + \overline{U}_n(t) \cos(\Delta_n a') + u_n(t) \sin(\lambda_n \varepsilon) \right] \tag{5}$$

$$w_p = \sum_{n=1}^{\infty} w_n(t) \sin(\gamma_n \varepsilon) \tag{6}$$

For the pipe bottom:

$$u_{pb} = \sum_{n=1}^{\infty} \left[U_n(t) \sin(\Lambda_n L') + \overline{U}_n(t) \cos(\Delta_n a') + u_n(t) \sin(\lambda_n \ell') \right] \tag{7}$$

The $U_n(t)$, $V_{rn}(t)$, $W_{rn}(t)$, $\overline{U}_n(t)$, $u_n(t)$, and $w_n(t)$ are the generalized time varying coordinates that describe the structural displacements. These will be called the generalized displacements.

Asymmetric breathing of the tank is allowed by the choice of v_t and w_t above. However, only axisymmetric breathing of the pipe has been prescribed, because asymmetric breathing is assumed to be a second order effect in the pipe.

The displacements prescribed above are used to calculate the strain energy in the structure in terms of the generalized displacements. This strain energy will then be substituted into Lagrange's equation.

The kinetic energy of the structure in terms of the generalized velocities will also be required in Lagrange's equation. To find this kinetic energy, the velocities of all points in the structure are calculated as the time derivatives of the displacements. A typical velocity equation is

$$\dot{u}_t = \sum_{n=1}^{\infty} \dot{U}_n(t)\sin(\Lambda_n \S) \tag{8}$$

where $\dot{U}_n(t)$ is a generalized velocity.

Kinetics of the Liquid

Laplace's equation (ref. 16) governs the motion of the incompressible, inviscid liquid. In terms of the nondimensionalized coordinates it is

$$\frac{1}{\eta}\frac{\partial \phi}{\partial \eta} + \frac{\partial^2 \phi}{\partial \eta^2} + \frac{1}{\eta^2}\frac{\partial^2 \phi}{\partial \theta^2} + \frac{\partial^2 \phi}{\partial \S^2} = 0 \tag{9}$$

where ϕ is the velocity potential function.

The solution of equation (9) is accomplished by assuming that the velocity potential function has the product form shown below and then applying standard separation of variables techniques.

$$\phi(\eta,\theta,\S,t) = N(\eta,t)\Theta(\theta,t)X(\S,t) \tag{10}$$

The complete solution of equation (9) is

$$\phi = \sum_{s=0}^{\infty} \left\{ \sum_{i=0}^{\infty} \left[A_{si}(t)\sin(K_{si}\S) + B_{si}(t)\cos(K_{si}\S) \right] I_s(K_{si}\eta) \right.$$

$$+ \sum_{j=0}^{\infty} \left[D_{sj}(t)\sinh(k_{sj}\S) + E_{sj}(t)\cosh(k_{sj}\S) \right] J_s(k_{sj}\eta)$$

$$\left. + \left[G_s(t) + \S\, H_s(t) \right] \eta^s \right\} \cos(s\theta) \tag{11}$$

J_s and I_s are respectively Bessel functions and modified Bessel functions of the first kind of order s. Neither the Bessel function nor the modified Bessel functions of the second kind appear in equation (11), because of their singularities at $\eta = 0$ which is an admissible point in our system.

Rather than use one velocity potential function, ϕ, for all of the liquid in the system, it is more convenient to consider a ϕ_t for the tank liquid and a ϕ_p for the pipe liquid. Both ϕ_t and ϕ_p have the form of equation (11), each having its own set of constants of integration such as $A_{si}(t)$. These constants of integration are determined from the following boundary conditions:

1. $\dot{w}_t = - \dfrac{1}{R} \dfrac{\partial \phi_t}{\partial \eta} \bigg|_{\eta=1}$

2. $\dot{w}_p = - \dfrac{1}{a} \dfrac{\partial \phi_p}{\partial \sigma} \bigg|_{\sigma=1}$

3. $\dot{u}_{tb} = - \dfrac{1}{R} \dfrac{\partial \phi_t}{\partial \S} \bigg|_{\S=L'}$

4. $\dot{u}_{pb} = - \dfrac{1}{a} \dfrac{\partial \phi_p}{\partial \epsilon} \bigg|_{\epsilon=\ell'}$

5. $\left(\dfrac{\partial^2 \phi_t}{\partial t^2} + \dfrac{g}{R} \dfrac{\partial \phi_t}{\partial \S} \right) \bigg|_{\S=L'-H'} = 0$

6. $\int_A P_t\, dA \bigg|_{\S=L'} = \int_A P_p\, dA \bigg|_{\epsilon=0}$

Boundary conditions 1 through 4 insure contact between the liquid and the structure at the tank wall, pipe wall, tank bottom, and pipe bottom respectively. In boundary condition 3, a negligible exchange of liquid between the tank and pipe is assumed.

Boundary condition 5 applies to the free surface (ref. 17) condition of the liquid. In applying this free surface condition, the ullage gas dynamic pressures are assumed to be small compared to the static pressure, p_O. Essentially, this implies that the dynamic pressures have negligible influence on the shape of the liquid surface waves.

In boundary condition 6 the total hydrostatic force at the top of the pipe is the same when calculated using either the pressure in the tank or pipe. This is a simplification over requiring the pressure at each point at the top of the pipe to be the same in both the tank and pipe.

The resulting equation for ϕ_t is

$$\frac{\phi_t}{R} = (L' - H' - \frac{1}{\alpha_t} - \S) \sum_{n=1}^{\infty} \dot{U}_n(t) \sin(\Lambda_n L')$$

$$+ \sum_{r=0}^{\infty} \sum_{n=1}^{\infty} \{ h_1(r,n) \sin(\Gamma_n \S) I_r(\Gamma_n \eta) + \sum_{j=0}^{\infty} h_2(r,j,n) \sinh(k_{rj} \S)$$

$$+ h_3(r,j,n) \cosh(k_{rj} \S) J_r(k_{rj} \eta) \} \cos(r\theta) \dot{W}_{rn}(t) \tag{12}$$

$$+ \sum_{n=1}^{\infty} \sum_{j=0}^{\infty} \left[h_5(j,n) \sinh(k_{oj} \S) + h_7(j,n) \cosh(k_{oj} \S) \right] J_0(k_{oj} \eta) \dot{\overline{U}}_n(t)$$

The functions $h_1(r,n)$ through $h_7(j,n)$ in equation (12) are listed in Appendix A, which is a listing of reference equations.

Similar equations for ϕ_p are also listed in Appendix A.

The kinetic energy of the liquid in terms of the generalized velocities will be required in Lagrange's equation. To find this kinetic energy, the velocity component in the n direction, $\dot{q}_n$, at each point in the liquid is calculated by the equation (ref. 16)

$$\dot{q}_n = - \frac{\partial \phi}{\partial n} \tag{13}$$

When ϕ_t or ϕ_p are substituted into equation (13) the velocity components are found in terms of the generalized velocities, $\dot{U}_n(t)$, etc.

11

Kinematics of the Ullage Gas

Although the actual motion of the gas is three dimensional, it is its longitudinal motion that primarily affects the longitudinal vibrations of the system. Therefore, the displacement of any point in the gas is assumed to be one-dimensional as follows,

$$u_g = \sin \frac{\pi \S}{2(L'-H')} \left\{ \sum_{n=1}^{\infty} U_n(t) \sin(\Lambda_n L') - 2 \sum_{n=1}^{\infty} \frac{(-1)^n}{\Gamma_n} (1 - \cos \Gamma_n H') W_{on}(t) \right.$$

$$\left. - 2 \sum_{n=1}^{\infty} \frac{1}{\Lambda_n^2} \left[1 + (-1)^n \Lambda_n \right] \bar{U}_n(t) \right\} + \sum_{n=1}^{\infty} \sin \frac{n\pi \S}{L'-H'} Q_n(t) \qquad (14)$$

The $Q_n(t)$ are new generalized displacements which account for the one-dimensional acoustic waves that travel between the liquid surface and the top of the tank.

The other terms in equation (14) account for the one-dimensional displacements of the gas caused by the longitudinal motion of the liquid averaged over its free surface. This average displacement is determined as follows: (1) the longitudinal velocity at any point in the liquid is obtained by substituting the ϕ_t of equation (12) into equation (13), where n is the axial direction; (2) when $\S = L'-H'$, the velocity on the free surface is found; (3) then this velocity is integrated with respect to time to find the displacement; and (4) the displacements are integrated over the area of the free surface and divided by πR^2.

From the gas displacement function of equation (14), the dilatation at any point in the gas will be calculated. Because the dilatation changes very rapidly, it is assumed that little heat transfer can occur and the process is adiabatic (ref. 18). The total potential energy in the gas, which will be needed in Lagrange's equation, is found from the dilatation (ref. 19).

The longitudinal velocity in the gas, which is found from the time derivative of u_g, is a function of the generalized velocities $\dot{U}_n(t)$, $\dot{W}_{on}(t)$, $\dot{\bar{U}}_n(t)$, and $\dot{Q}_n(t)$. The kinetic energy of the gas is found from this velocity function for substitution into Lagrange's equation.

Equations of Motion

Lagrange's equation (ref. 20) for the unforced vibrations of this system is

$$\frac{d}{dt} \left(\frac{\partial T}{\partial \dot{q}_i} \right) + \frac{\partial V}{\partial q_i} = 0 \qquad i = 1, 2, 3, \ldots \tag{15}$$

where T is the total kinetic energy and V is the total potential energy of the system. The symbols q_i and $\dot{q}_i$ represent the generalized displacements and the generalized velocities respectively.

The total kinetic energy of the system is the sum of the kinetic energies of each component, or

$$T = T_t + T_{tb} + T_p + T_{pb} + T_\ell + T_g \tag{16}$$

The total potential energy of the system is the sum of the potential energies of each component, or

$$V = V_t + V_{tb} + V_p + V_g \tag{17}$$

Since the displacements are measured from the static equilibrium configuration of the system, the potential energy associated with the longitudinal (vertical) displacement of weight is cancelled by the change in strain energy associated with the stresses at equilibrium. For this reason the strain energy of the structure is referred to a zero value at equilibrium and no potential energy associated with the weight of the structure, liquid, or gas is included. Therefore, the first three terms in equation (17) are the strain energies of the tank, tank bottom, and pipe respectively. The last term is the potential energy in the gas due to its dilatation. The liquid has no potential energy because it is incompressible.

Each kinetic energy component in equation (16) and each potential energy component in equation (17) is an integral. All of these integrals are listed in Appendix B.

Equation (15) is written once for each generalized displacement and corresponding generalized velocity. For instance, for U_1 and $\dot{U}_1$ it is

$$\frac{d}{dt} \left(\frac{\partial T}{\partial \dot{U}_1} \right) + \frac{\partial V}{\partial U_1} = 0 \tag{18}$$

When equations (16) and (17) are substituted into equation (18), there results six kinetic energy derivative and four potential energy derivative terms.

For instance, the kinetic energy of the tank cylinder is

$$T_t = \frac{\rho_t R^2 h_t}{2} \int_0^{L'} \int_0^{2\pi} (\dot{u}_t^2 + \dot{v}_t^2 + \dot{w}_t^2)\, d\theta\, d\S \tag{19}$$

where ρ_t is the mass density of the tank material. The partial derivative is

$$\frac{\partial T_t}{\partial \dot{U}_1} = \rho_t R^2 h_t \int_0^{L'} \int_0^{2\pi} \{\dot{u}_t \frac{\partial \dot{u}_t}{\partial \dot{U}_1} + \dot{v}_t \frac{\partial \dot{v}_t}{\partial \dot{U}_1} + \dot{w}_t \frac{\partial \dot{w}_t}{\partial \dot{U}_1}\}\, d\theta\, d\S \tag{20}$$

Since $\dot{u}_t$, $\dot{v}_t$, and $\dot{w}_t$ are linear functions of the generalized velocities, then equation (20) is also linear in these generalized velocities. The term $\frac{d}{dt}(\frac{\partial T_t}{\partial \dot{U}_1})$ is obtained by differentiating equation (20) and is a linear function of the generalized accelerations, such as $\ddot{U}_1$, $\ddot{U}_2$, $\ddot{W}_{01}$, $\ddot{u}_1$, etc. Assuming the motion of the system is simple harmonic, the generalized acceleration can be replaced by the negative of ω^2 times the corresponding generalized displacement. For instance

$$\ddot{U}_1 = -\omega^2 U_1 \tag{21}$$

Therefore, the term $\frac{d}{dt}(\frac{\partial T_t}{\partial \dot{U}_1})$, which is one of the contributions to the first term of equation (18), involves ω^2 and linear combinations of the generalized displacements.

Similarly, the strain energy of the plate bottom is

$$V_{tb} = \frac{\pi D_{tb}}{R^2} \int_{a'}^1 \{(\frac{d^2 u_{tb}}{d\eta^2})^2 - \frac{1-\mu}{2\eta} \frac{du_{tb}}{d\eta} \frac{d^2 u_{tb}}{d\eta^2} + \frac{2-\mu}{2\eta^2}(\frac{du_{tb}}{d\eta})^2 \}\eta\, d\eta \tag{22}$$

Equation (22) involves the squares and products of the generalized displacements. The equation for $\frac{\partial V_{tb}}{\partial U_1}$, which is one of the contributions to the second term of equation (18), is linear in the generalized displacements.

Many kinetic energy derivatives, such as $\frac{d}{dt}(\frac{\partial T_t}{\partial \dot{U}_1})$, and po-

tential energy derivatives, such as $\frac{\partial V_{tb}}{\partial U_1}$, are substituted into

equation (18) to produce an equation of the form

$$f_1(q_i) + \omega^2 g_1(q_i) = 0 \tag{23}$$

where $f_1(q_i)$ and $g_1(q_i)$ are linear functions of the generalized displacements.

Equation (23) is Lagrange's equation for the generalized displacement, U_1. One equation for each generalized displacement is formulated and a set of simultaneous equations of the following form is generated

$$f_j(q_i) + \omega^2 g_j(q_i) = 0 \tag{24}$$

Equation (24) can be written in matrix notation as

$$[A]\{q\} = \omega^2 [B]\{q\} \tag{25}$$

where $[A]$ and $[B]$ are square matrices and $\{q\}$ is a column matrix of the generalized displacements.

General Characteristic Value Equation

Equation (25) governs the unforced vibrations of the system. It is a general characteristic value equation (ref. 21), whose solution furnishes the natural frequencies of the system as the characteristic values and the corresponding mode shapes as the characteristic functions.

In the Rayleigh-Lagrange analysis, accuracy is improved by using more generalized coordinates to approximate the motion of the continuous solution. Therefore, the matrices are of large order. Also the individual elements in the A and B matrices are very complicated and involve lengthy calculations. For these reasons, the solution of equation (25) has been programed for a digital computer.

COMPUTER PROGRAM

A computer program has been developed that will determine the frequencies and mode shapes for any system consistent with Figure 1 and the assumptions previously stated. The program is written in Fortran IV language and is executed on an IBM 360/50 computer. The flow chart is presented in Appendix C.

Any numerical values for the dimensions of the system and the physical properties of the structural materials, the liquid and the gas may be used as input. The specification of the number and types of generalized displacements is also required as input to the program.

The program uses the input to calculate the individual elements of the A and B matrices in equation (25). Then a subroutine finds the characteristic values and functions, frequencies and mode shapes, by using a Jacobi (ref. 22) matrix diagonalization technique.

The output of the computer program consists of the frequencies and corresponding mode shapes for the system at all liquid heights, H, which were specified in the input data. One frequency and corresponding mode shape is obtained for each generalized displacement specified in the input. The frequencies, in Hz, are printed in ascending order and the corresponding mode shapes, which are normalized to produce a maximum generalized displacement equal to unity, are printed next in the same order. The input data and generalized displacements specified are also printed in a convenient format. A typical computer printout is shown in Appendix C.

After the program has been compiled, each data point is executed in a few seconds up to about two minutes, depending on the number and types of generalized displacements specified in the input. In the analysis, a modified Schwarz integral of the form

$$Z_1(j,m) = \int_0^1 \eta \, J_0(k_{oj}\eta) \, \cos(\Delta_m \eta) d\eta$$

is encountered. Instead of using a subroutine in this computer program to calculate the values of $Z_1(j,m)$ for each data point, a table of values was generated using Simpson's Rule in a separate computer program and the values were read into this program. This represents a substantial saving of execution time for each data point. The zeros of J_r' are also needed and were read into the program in preference to using a subroutine. This also reduces the execution time.

16

A plotter program has been developed to produce a graph of the two lowest frequencies versus liquid height. If a plot is desired, the punched output cards of the computer program **are** used in the plotter program, which draws the graph with the axes annotated and the system properties listed. A typical computer plot is included in Appendix C.

INFLUENCE OF THE GENERALIZED DISPLACEMENTS ON THE SYSTEM RESPONSE

Discussion

The computer program facilitates the study of many configurations of the basic system shown in Figure 1. It also permits the selection of a large number of generalized displacements for increased accuracy of the frequencies and mode shapes obtained by the Rayleigh-Lagrange method. However, care must be exercised in the types of generalized displacements selected as well as in their number. Because the motion being studied is longitudinal, it is reasonable to select many longitudinal generalized displacements, such as $U_n(t)$, $\overline{U}_n(t)$, $u_n(t)$, and $Q_n(t)$. Since breathing can influence the longitudinal motion, generalized displacements such as $V_{rn}(t)$, $W_{rn}(t)$, and $w_n(t)$ should also be selected, but in smaller numbers.

The system, whose dimensions are shown in Figure 2, will be used to study the influence of the generalized displacements specified in the computer program on the frequencies calculated. This system, which is made of aluminum and contains water and air at atmospheric pressure, was tested at NASA Langley Research Center by Harold B. Pierce. These were preliminary tests to determine the frequencies in the range expected from an approximate analysis of its longitudinal vibrations. Hereafter, this system will be called the
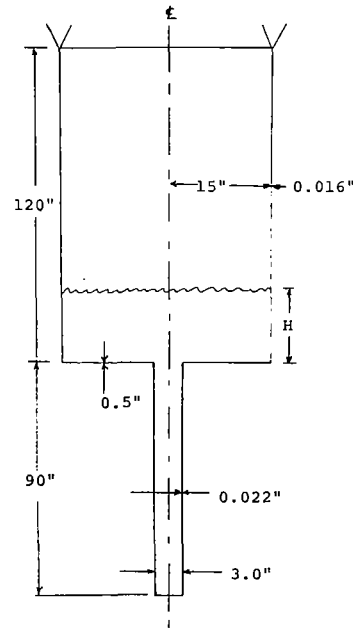

Figure 2.
Standard Configuration

17

"standard configuration".

The frequencies for the standard configuration will be determined from several computer runs, each of which contain different combinations of generalized displacements. These runs will be of increasing complexity to evaluate the influence of each type of generalized displacement on the calculated frequencies.

First the system will have a rigid tank bottom, no ullage gas effects, and only axisymmetric breathing. This is accomplished by assigning values of zero to the $\bar{U}_n(t)$ terms, the gas density and bulk modulus, and the subscript r respectively.

Next the tank bottom will be made flexible by selecting some nonzero $\bar{U}_n(t)$ terms.

Then the effect of the ullage gas is considered by selecting nonzero gas density and bulk modulus and nonzero $Q_n(t)$ terms. For this study the tank bottom is made rigid again by assigning zero to the $\bar{U}_n(t)$ terms.

In the next run the ullage gas effects are included and the tank bottom is also made flexible.

Finally the effect of asymmetric breathing is evaluated by letting the subscript r be nonzero.

The purpose of these studies is to determine the relative importance of the different types of generalized displacements on the calculated frequencies. The experimental frequencies will then be compared to the computed frequencies to evaluate the effectiveness of the different methods of selecting the generalized displacements.

Rigid Tank Bottom - No Ullage Gas

The generalized displacements selected for this computer run are U_1, U_2, U_3, W_1, W_2, W_3, u_1, u_2, u_3, and w_1. Note that when r = 0, all terms in $V_{rn}(t)$ disappear and the $W_{rn}(t)$ terms can be written as $W_n(t)$.

The three lowest frequencies versus liquid height, H, are shown in Figure 3.

18

The uncoupled frequency of
the pipe is approximately 85 Hz
and the uncoupled frequency of
the tank varies inversely with
the square root of the liquid
height from approximately 163 to
16 Hz. These are shown by
dotted lines in Figure 3.

The tank motion is relative-
ly uncoupled from 10 to 120
inches as shown by the lowest
curve. It would follow the
dotted curve between 0 and 10
inches if it remained uncoupled.
However, it couples strongly with
the pipe in this region.

In the 35 to 70 inch range
the pipe is also coupled with
tank breathing, which is the
second lowest curve at high
liquid heights and the highest
curve below 50 inches. The pipe
is also coupled with another
breathing mode in the 90-120
inch range.

Thus, the axisymmetric
breathing can be seen to have a
considerable influence on the
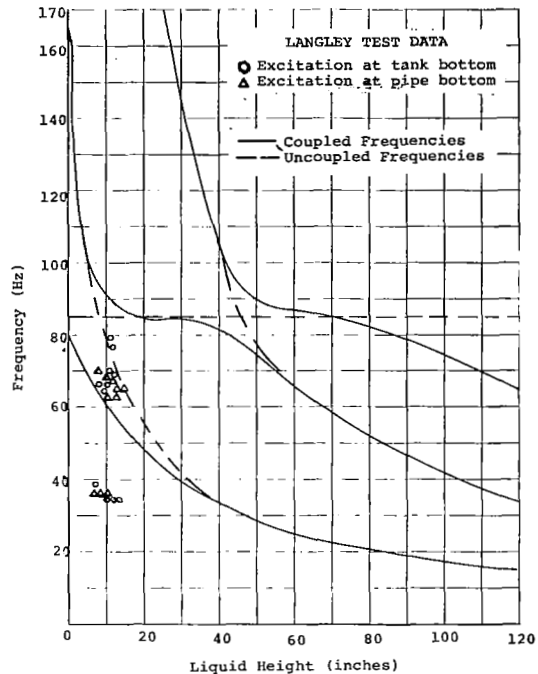longitudinal frequencies of the
system.

Figure 3.
Rigid Bottom - No Ullage Gas

Flexible Tank Bottom - No Ullage Gas

The generalized displacements selected for this computer run

are U_1, U_2, U_3, W_1, W_2, W_3, $\overline{U}_1$, $\overline{U}_2$, $\overline{U}_3$, u_1, u_2, u_3, and w_1.

The three lowest frequencies versus liquid height are shown
on Figure 4. For reference the curves of Figure 3 are shown
dotted on Figure 4.

The lowest curve corresponds primarily to the motion of the
tank bottom. However, the tank bottom also couples strongly with
the other motions.

Due to coupling with the tank bottom, the tank frequency

19

curve is raised and now couples with the pipe in the 0 to 40 inch range.

The pipe motion is so highly coupled that it is virtually indistinquishable in Figure 4.

The tank breathing curve is also raised in the 40 to 120 inch region due to coupling with the tank bottom.

The most significant effect of including the flexibility of the tank bottom is the lowering of the fundamental frequency of the system. The other frequencies are also changed significantly due to increased coupling.

Rigid Tank Bottom with Ullage Gas

The generalized displacements selected for this computer run are U_1, U_2, U_3, W_1, W_2, u_1, u_2, u_3, w_1, Q_1, Q_2, Q_3, Q_4, and Q_5.
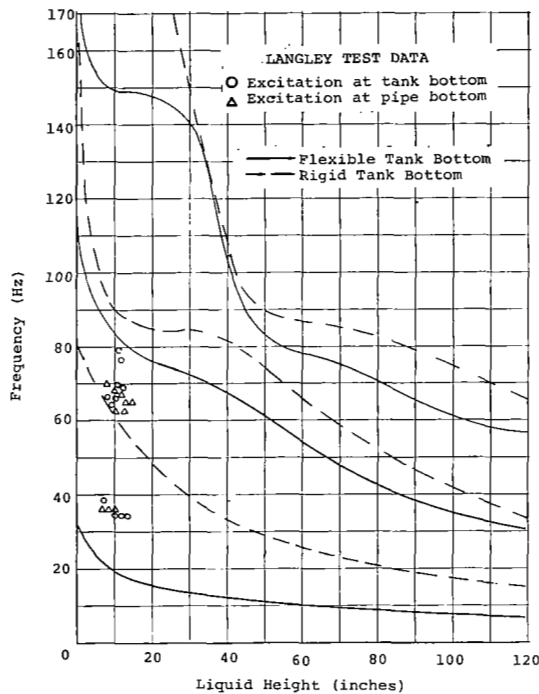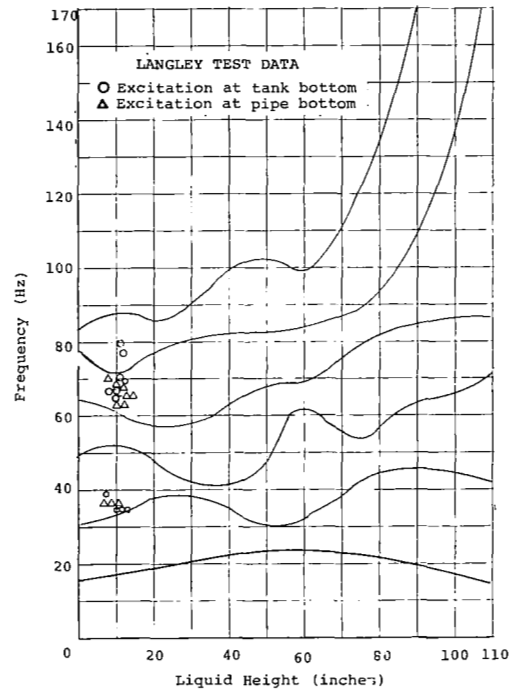
Figure 4.
Flexible Bottom – No Ullage Gas

Figure 5.
Rigid Bottom With Ullage Gas

20

The bulk modulus is 21 pounds per square inch and the gas density is 1.376×10^{-6} slugs per cubic inch. These correspond to the air at atmospheric pressure of Langley's experiment.

The six lowest frequencies versus liquid height are shown on Figure 5.

These frequency curves are quite different from those of Figure 3 where the ullage gas was not considered. However, any one curve is composed of structure motion at certain liquid heights and acoustic wave motion at other liquid heights. For instance, the lowest frequency curve corresponds to acoustic motion from 0 to about 60 inches and tank motion from 60 to 110 inches.

In Figure 6 the frequencies of the pure acoustic waves are shown as dotted lines and the structural frequencies from Figure 3 are shown solid. Where these curves cross in Figure 6 there is coupling and the coupled curves pass above and below the inter-
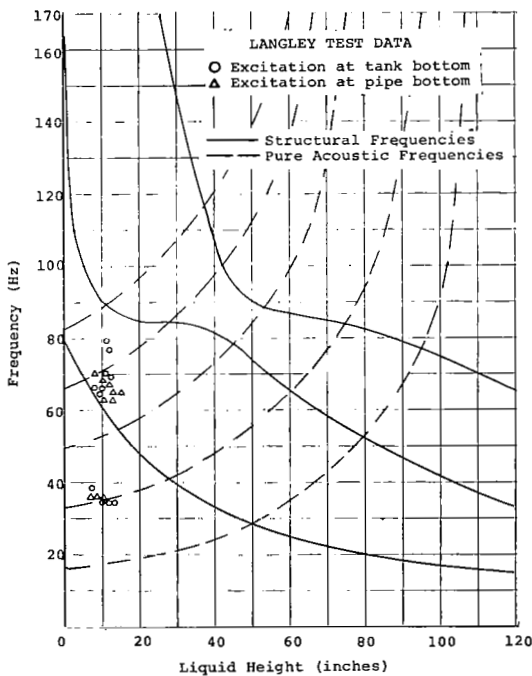

Figure 6.
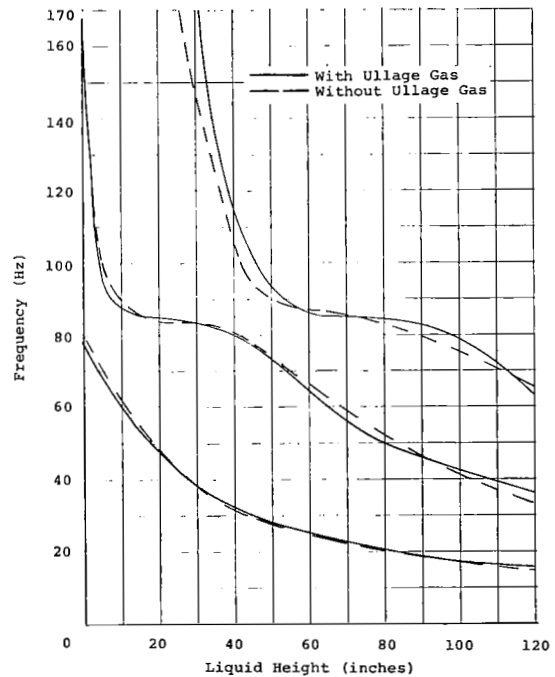Separate Structural
and Acoustic Modes

Figure 7.
Structural Modes
with Acoustic Effects

21

sections. In this manner the curves of Figure 6 can be correlated to those of Figure 5.

Therefore, the frequencies corresponding primarily to structural motions are only changed at certain liquid heights where they are coupled with the acoustic waves. The solid curves in Figure 7 show the structural frequencies as altered by the acoustic waves. The dotted curves in Figure 7 are identical to Figure 3 where no ullage gas is considered.

As may be seen from Figure 7, the ullage gas has only a small effect on the structural frequencies. However, numerous acoustic wave frequencies are also present. For the case of forced vibrations, the ullage gas can have infinite impedance at certain forcing frequencies, and reduce the amplitude of the structural motion to zero (ref. 23).
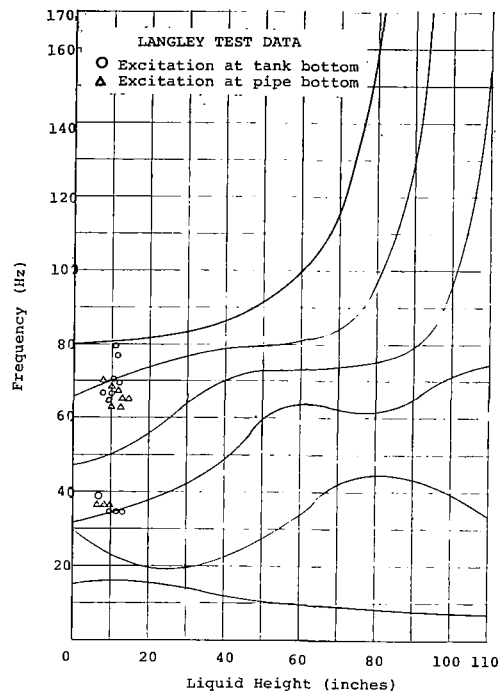
Figure 8.
Flexible Bottom with Ullage Gas

Flexible Tank Bottom with Ullage Gas

The generalized displacements selected for this computer run are U_1, U_2, U_3, W_1, $\overline{U}_1$, $\overline{U}_2$, $\overline{U}_3$, u_1, u_2, w_1, Q_1, Q_2, Q_3, Q_4, and Q_5. The gas properties are the same as the previous computer run.

The six lowest frequencies versus liquid height are shown on Figure 8.

In general, the results are similar to those where the tank bottom is rigid. The frequency curves are made up of the structural frequency curves and the acoustic wave curves with coupling at certain liquid heights. Again the structural frequencies are only affected to a small extent by the ullage gas. Also, as before, numerous acoustic wave frequencies are also present and they may have infinite impedance at certain forcing frequencies.

22

Asymmetric Breathing

When some asymmetric breathing terms are added to a previous axisymmetric computer run, the new list of frequencies and mode shapes contain those of the axisymmetric case plus new uncoupled frequencies and mode shapes that correspond to the asymmetric breathing. Therefore, asymmetric breathing has no effect on the longitudinal frequencies and mode shapes of the system, because a linear analysis is used.

The cross sectional area of the tank at any longitudinal station is not altered by asymmetric breathing, because there is as much area subtracted due to inward radial displacements as is gained from outward radial displacements. Thus for asymmetric breathing, there is no tendency for the liquid to rise or fall due to cross sectional area change. This is obviously not the case for axisymmetric breathing. Therefore, the conclusion that axisymmetric breathing does and asymmetric breathing does not affect the longitudinal frequencies is physically reasonable.

Comparison of Experimental and Calculated Frequencies

The Langley experiments on the standard configuration were performed only for low liquid levels, up to approximately 15 inches. The experimental frequencies are shown as data points on Figures 3, 4, 5, 6, and 8. Circled data points are the frequencies for excitation of the system at two diametrically opposite points on the bottom edge of the tank. Triangle data points are the frequencies for excitation of the system at the bottom of the pipe. There are small discrepancies between the frequencies determined by the two methods of excitation.

As can be seen in Figures 3 and 4, the general correlation is poor when no ullage gas effects are included. Many of the experimental data points are completely uncorrelated with the curves.

In Figure 6 most experimental points correlate with the curves that are primarily acoustic wave motion. The experimental points near 80 Hz do not correlate with any curve.

In Figure 8 all of the experimental points correlate with the curves. The two lower sets of points are primarily acoustic wave motion and the points near 80 Hz are primarily structural motion. The 80 Hz points also correlated in Figure 4 where no ullage gas effects were considered.

Pierce noted that the experimental frequencies near 35 Hz were "full of harmonics". The 35 Hz frequency is the first har-

monic acoustic wave, while the other harmonic frequencies noted
by Pierce are the fundamental at about 18 Hz plus all the other
harmonics of the acoustic waves. This can be observed on Figure
6.

Except for the frequencies near 80 Hz, most of the experi-
mental frequencies found were associated with acoustic wave
motion. The fundamental structural motion of the system, which
is primarily tank bottom bending, was not observed experimentally,
because the tests were conducted above this frequency.

INFLUENCE OF GEOMETRY ON SYSTEM RESPONSE

Discussion

In this section the influence of changing dimensions from
those of the standard configuration will be investigated. One
dimension will take on different values while all others remain
standard. The frequencies will be determined at all liquid
heights for each value of that dimension. This procedure will be
repeated using different dimensions as the nonstandard value.

No ullage gas effects will be included in these investi-
gations, because the structural frequencies are masked by these
effects. Only the changes in the fundamental frequency will be
presented.

Rigid Tank Bottom - No Ullage Gas

The frequency versus liquid
height curves for variations of
the tank radius, the tank wall
thickness, the pipe length (or
pipe radius), and the pipe wall
thickness are shown in Figures 9
to 12 respectively. In each
case the fundamental frequency
corresponds to the uncoupled
frequency of the tank above
about 30 inches with some pipe
coupling below 30 inches or less.

In Figure 9 an increase in
tank radius decreases the funda-
mental frequency, because the
mass of the liquid in the tank
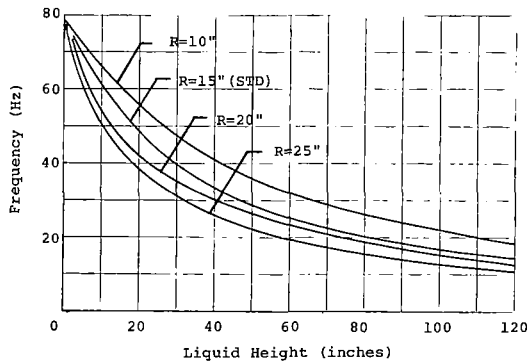is increased. At low liquid
heights the curves converge be-

Figure 9.
Variable Tank Radii

24

cause of coupling with the pipe.

An increase of tank wall thickness increases the fundamental frequency as shown in Figure 10, because the tank stiffness is increased. Again the curves tend to converge at low liquid levels because of pipe coupling.

An increase of the pipe length (or pipe radius) decreases the uncoupled pipe frequency, because the pipe mass increases. This in turn causes the coupling between the tank and pipe to occur over a greater range of liquid heights. A decrease of pipe length (or pipe radius) will have the opposite effect. For instance, coupling is almost eliminated for ℓ = 60" as shown in Figure 11.

Decreasing the pipe wall thickness decreases the uncoupled pipe frequency, because the pipe stiffness decreases. This again causes the coupling to occur over a greater range of liquid heights as shown in Figure 12.
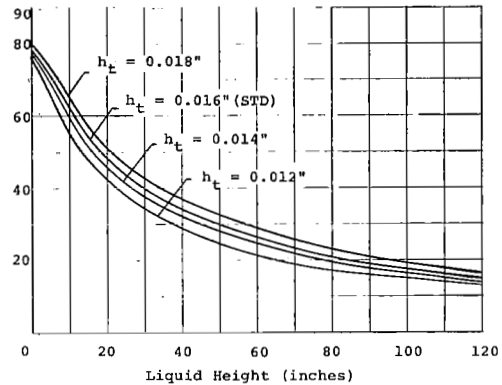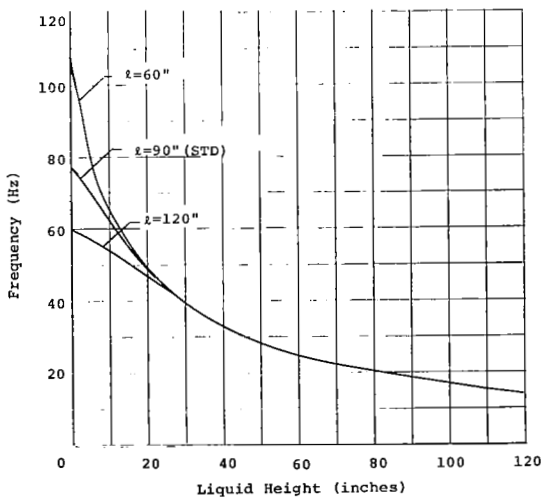
Figure 10.
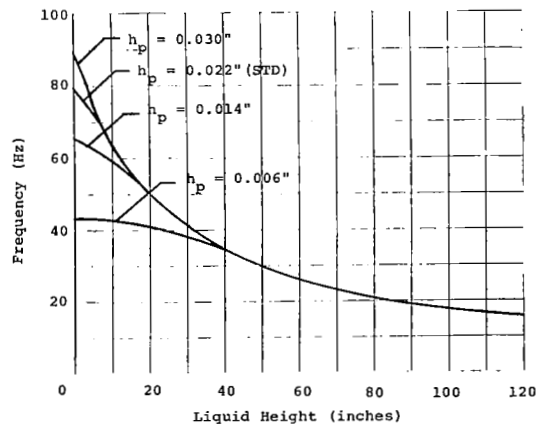Variable Tank Wall Thickness

Figure 11.
Variable Pipe Lengths

Figure 12.
Variable Pipe Wall Thickness

25

Flexible Tank Bottom - No Ullage Gas

The frequency versus liquid height curves for variations of the tank bottom thickness, tank radius, and pipe length (or pipe radius) are shown in Figures 13 to 15 respectively. In each case the fundamental frequency corresponds primarily to the motion of the tank bottom.

An increase in the tank bottom thickness stiffens the tank bottom and raises the fundamental frequency as shown in Figure 13.

An increase in tank radius increases the mass of liquid in the tank, which must be supported by the tank bottom, and also decreases the bending stiffness of the tank bottom. Both of these effects tend to lower the fundamental frequency as shown in Figure 14.

Changes in the pipe length (or pipe radius) at high liquid heights have no effect on the fundamental frequency, because the slight change in mass of the liquid in the pipe compared to the liquid in the tank is insignificant. However, at low liquid levels the pipe liquid becomes comparable to the tank liquid, and the mass supported by the tank bottom is significantly altered by changes in pipe length (or pipe radius). Increasing the pipe length (or pipe radius) increases the mass supported by the tank bottom, and decreases the fundamental frequency as shown in Figure 15.

Changes in the tank wall thickness have little effect on the fundamental frequency, because they do not change the liquid mass supported by the tank bottom or the tank bottom
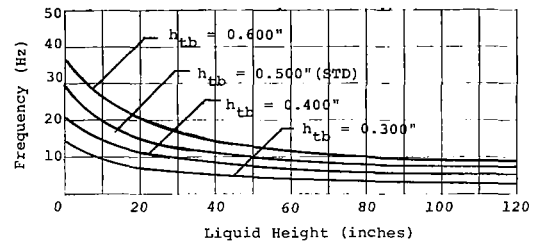

Figure 13.
Variable Tank Bottom Thickness
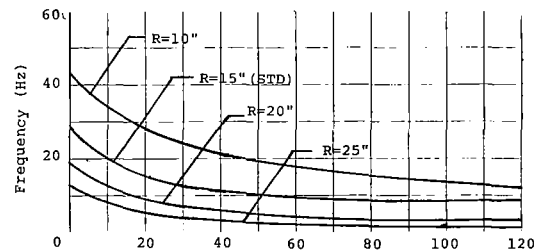
Figure 14.
Variable Tank Radii
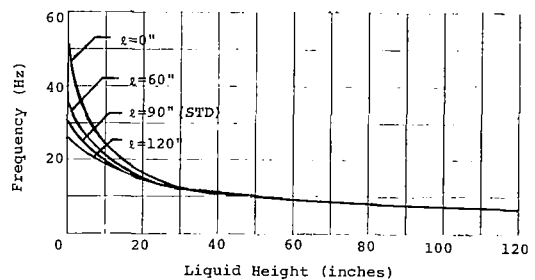
Figure 15.
Variable Pipe Lengths

26
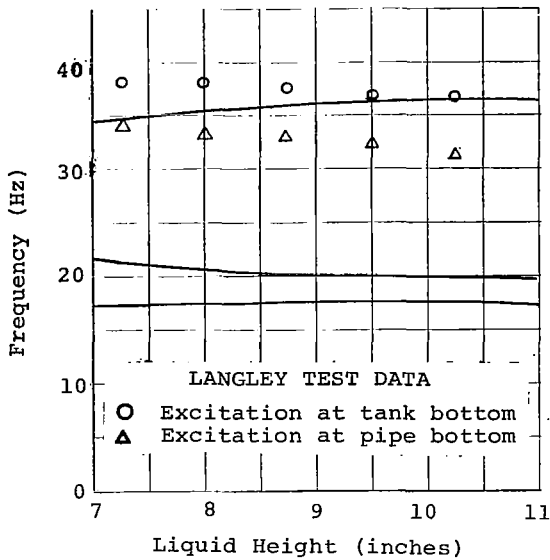
Figure 16.
Steel Pipe Configuration
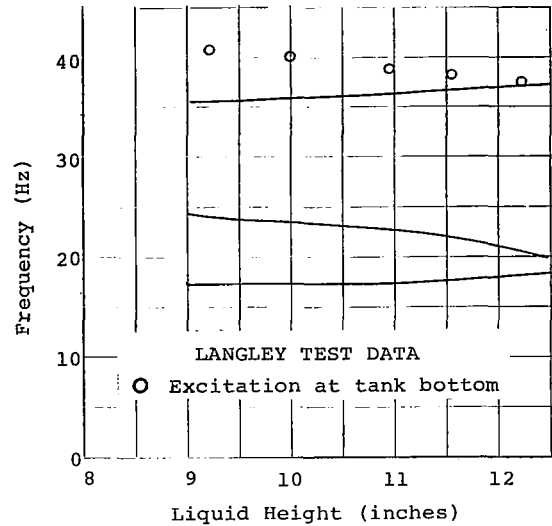
Figure 17.
No Pipe Configuration

stiffness. The changes of the uncoupled tank frequency do not affect the fundamental frequency, because they are uncoupled.

Changes in the pipe wall thickness have little effect on the fundamental frequency for the same reasons cited for changes in the tank wall thickness.

Comparison of Experimental and Calculated Frequencies

The experimental investigations conducted at Langley Research Center by Pierce included two geometries other than the standard configuration. The first used a steel pipe with a wall thickness of 0.12", instead of an aluminum pipe. The second had no pipe. These tests were also performed only for low liquid levels, up to approximately 15 inches.

Computer runs were made for these two configurations including the effects of a flexible tank bottom and the ullage gas. The computed frequencies for the steel pipe configuration are shown in Figure 16 with the experimental data shown by circled and triangle points as defined on page 23. Similar curves and experimental data for the no pipe configuration are shown on Figure 17. The correlation between the calculated and experimental frequencies is satisfactory.

PARAMETRIC STUDIES OF SYSTEM RESPONSE

Discussion

Certain combinations of system dimensions and physical properties can be grouped together to form parameters. All systems having the same numerical values of all parameters constitute a family having essentially identical system responses.

In this section these parameters will be identified and computer calculations will be used to check their validity.

The computer program uses individual dimensions and physical properties rather than parameters as input. No attempt has been made to change the input format to accept the parameters. Once the validity of the parameters has been proven, the program can be run using dimensions which yield the desired values of the parameters and these runs are valid for all systems having the same values of the parameters.

Definition of System Parameters

It is reasonable to expect all systems that have identical uncoupled frequencies of each component and also the same ratio of masses of the components to be members of the same family and have identical frequency responses.

Therefore, it is postulated that a family of systems, which have the basic configuration shown in Figure 1, have practically identical frequency curves when the following conditions are satisfied:

1. The mass ratios of the liquid in the tank to the liquid in the pipe to the ullage gas are the same for all systems.

2. The ratios of the stiffness of the tank to the pipe to the tank bottom to the ullage gas are the same for all systems.

3. The ratio of the stiffness divided by the mass, that is the square of the uncoupled natural frequency, of each of the tank, pipe, tank bottom, and ullage gas are the same for all systems.

Obviously, if any two of the above conditions are satisfied, then the remaining condition is automatically satisfied.

The approximate stiffnesses of the tank, pipe, tank bottom, and ullage gas respectively are proportional to

$$k_t = \frac{Eh_t R}{L} \;, \quad k_p \simeq \frac{Eh_p a}{\ell} \;, \quad k_{tb} \simeq \frac{Eh_{tb}^3}{R^4} \;, \quad k_g \simeq \frac{B}{L-H} \;.$$

Since only ratios of the stiffnesses are required, it is only necessary to define each stiffness to within a constant of proportionality. The approximate stiffnesses of the tank, pipe, and ullage gas have been determined from a one dimensional analysis. The stiffness of the tank bottom is its flexural stiffness.

The mass of the tank bottom is assumed to be the mass of the liquid in the system, because it is all supported by the tank bottom. The mass of the tank bottom itself and of the ullage gas are considered negligible compared to that of the liquid.

Because approximations are involved in the stiffnesses and, to a lesser extent, the masses of each component of the system, the frequency responses of systems of a given family might not be identical. Therefore, several computer investigations have been performed to check the validity of the postulated criteria for parametric systems.

Parametric Studies

The response of the standard configuration has been thoroughly investigated in the section "Influence of the Generalized Displacements on the System Response". Therefore, the standard configuration will be used to establish the parameters of a family. The following parametric systems are also members of the same family according to the rules postualted above. The dimensions and properties listed below are the only ones changed from the standard configuration, except in all cases $B = 140$ and $\rho_g = .931$ x 10^{-5} were used. Each parametric system is designated by a letter as follows:

A: $h_p = .0073$, $E_p = 30 \times 10^6$. (symbol $\triangle$)

B: $\ell = 120$, $a = 1.3$, $h_p = .0338$. (symbol $\cdot$)

C: $E_t = E_p = E_{tb} = 30 \times 10^6$, $\rho_\ell = 2.8035 \times 10^{-4}$. (symbol o)

D: $h_t = .0053$, $h_{tb} = .3467$, $E_t = E_{tb} = 30 \times 10^6$. (symbol x)

E: $R = 10$, $a = 1$, $h_t = .0107$, $h_p = .0147$, $h_{tb} = .2911$.
(symbol *)

F: $R = 20$, $a = 2$, $h_t = .0213$, $h_p = .0293$, $h_{tb} = .7335$.
(symbol $\square$)

29

The results of these parametric studies are shown in Figures 18 through 20. On these figures the curves are for the standard configuration while the frequencies of the parametric systems are shown as data points having the symbols listed above. When several symbols are either at the same point or in very close proximity, only one symbol will be shown for clarity. In all cases the symbol that is in greatest disagreement with the solid curve will be shown.

Figure 18 shows the results for a rigid tank bottom with no ullage gas, Figure 19 for a flexible tank bottom with no ullage gas, and Figure 20 for a flexible tank bottom with the ullage gas effect. The dotted curves in Figure 20 are the pure acoustic wave frequencies, while the solid curves are the structural frequencies with acoustic effects analogous to the solid curves in Figure 7.
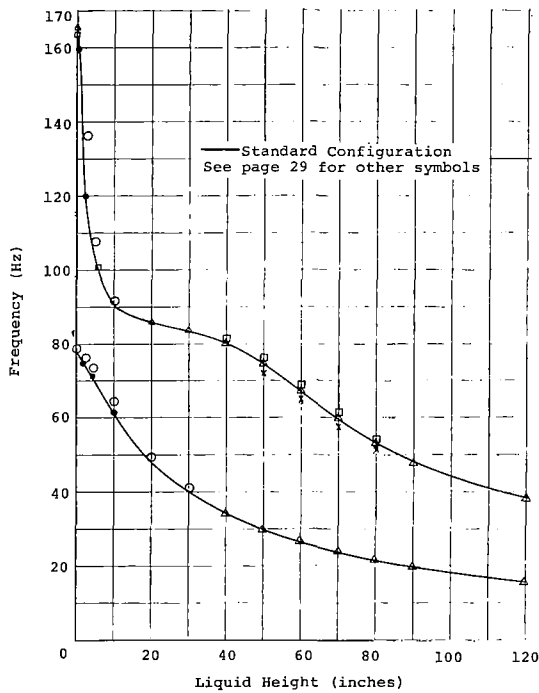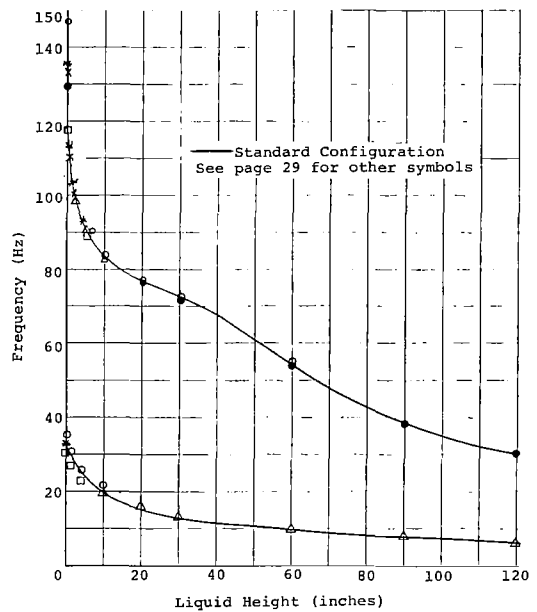

Figure 18.
Rigid Bottom - No Ullage Gas

Figure 19.
Flexible Bottom - No Ullage Gas

30

SUMMARY AND CONCLUSIONS

Summary

A Rayleigh-Lagrange solution has been developed and a computer program has been written for determining the unforced frequencies and mode shapes at all liquid heights for any system which has the general configuration shown in Figure 1.

Comparison of the experimental data with the calculated frequency curves clearly indicates that the flexibility of the tank bottom is important and should be included in the analysis. The structural frequencies correlated well with the experimental frequencies when the flexibility of the tank bottom was considered, even when the ullage gas effect was neglected. However, ullage gas effects must be included if the acoustic wave frequencies are to be determined. In addition, the acoustic waves couple with the structural motion to a small extent as shown in Figure 7.

Axisymmetric breathing should be included in the analysis, because at some liquid heights, it couples strongly with the longitudinal structural motion. Asymmetric breathing is completely uncoupled and should not be included in the analysis.

The effects of changing individual dimensions or physical properties of the system have been determined and are represented graphically in Figures 9 through 15. The trends represented quantatively in these figures are in agreement with qualitative trends obtained from physical considerations.

Parameters have been identified which define families of systems having practically identical frequencies at all liquid heights. It is concluded that the approximations made in the parametric studies do not seriously affect the accuracy of the parametric calculations.

Conclusions

The method developed herein for finding frequencies and mode shapes is accurate and tractable for the system being studied.

A fuel (or oxidizer) tank of a liquid fueled launch vehicle normally has some shell type bottom, rather than a flat plate. In this analysis, the effect of the tank bottom on the frequencies and mode shapes has been found to be very important. For this reason, the actual tank bottom configuration should be represented faithfully in future analyses.

APPENDIX A
Velocity Potential Function for Pipe

$$\frac{\phi_p}{a} = - \left(H'' + \frac{1}{\alpha_p} + \varepsilon\right) \sum_{n=1}^{\infty} \dot{U}_n(t) \sin(\Lambda_n L')$$

$$+ \frac{2R^2}{a^2} \sum_{n=1}^{\infty} \sum_{j=0}^{\infty} \left[h_2(0,j,n) \sinh(k_{oj}L') \right.$$

$$+ \left. h_3(0,j,n) \cosh(k_{oj}L') \right] \frac{1}{k_{oj}} J_1\left(\frac{k_{oj}a}{R}\right) \dot{W}_{on}(t)$$

$$+ \sum_{n=1}^{\infty} \left\{ -\varepsilon \cos(\Delta_n a') + \frac{2R^2}{a^2} \sum_{j=0}^{\infty} \left[h_5(j,n) \sinh(k_{oj}L') \right. \right.$$

$$+ \left. \left. h_7(j,n) \cosh(k_{oj}L') \right] \frac{1}{k_{oj}} J_1\left(\frac{k_{oj}a}{R}\right) \right\} \dot{\bar{U}}_n(t)$$

$$- \varepsilon \sum_{n=1}^{\infty} \dot{u}_n(t) \sin(\lambda_n \ell') + \sum_{n=1}^{\infty} \left[g_1(n) \sin(\gamma_n \varepsilon) I_o(\gamma_n \sigma) \right.$$

$$+ \sum_{j=0}^{\infty} \frac{2\gamma_n(-1)^n}{k_{oj}\cosh(k_{oj}\ell')J_o(k_{oj})(\gamma_n^2+k_{oj}^2)} \left. \sinh(k_{oj}\varepsilon)J_o(k_{oj}\sigma) \right] \dot{w}_n(t)$$

Definition of Functions Used in ϕ_t and ϕ_p Equations

$$h_1(r,n) = \frac{-1}{rI_r(\gamma_n)+\gamma_n I_{r+1}(\gamma_n)} = \frac{-1}{\gamma_n I_r'(\gamma_n)}$$

$$h_2(r,j,n) = \frac{2k_{rj}(-1)^n}{(k_{rj}^2-r^2)J_r(k_{rj})(\gamma_n^2+k_{rj}^2)} \left[\gamma_n \cosh(k_{rj}L') \right.$$

$$\left. -k_{rj}\sinh(k_{rj}L')h_4(r,j,n) \right]$$

$$h_3(r,j,n) = \frac{2k_{rj}(-1)^n}{(k_{rj}^2-r^2)J_r(k_{rj})(\gamma_n^2+k_{rj}^2)} \left[k_{rj}\cosh(k_{rj}L')h_4(r,j,n) \right.$$

$$\left. - \gamma_n \sinh(k_{rj}L') \right]$$

$$h_4(r,j,n) = \frac{1}{k_{rj}\sinh(k_{rj}H') + \alpha_t \cosh(k_{rj}H')} \left[\frac{\Gamma_n \alpha_t}{k_{rj}} \sinh(k_{rj}H') \right.$$

$$\left. + \Gamma_n \cosh(k_{rj}H') - \alpha_t \sin(\Gamma_n H') - \Gamma_n \cos(\Gamma_n H') \right]$$

$$h_5(j,n) = \frac{2Z_1(j,n)}{k_{oj}J_o^2(k_{oj})} \left[\sinh(k_{oj}L')h_6(j) - \cosh(k_{oj}L') \right]$$

$$h_6(j) = \frac{\alpha_t \sinh(k_{oj}H^*) + k_{oj}\cosh(k_{oj}H')}{k_{oj}\sinh(k_{oj}H') + \alpha_t \cosh(k_{oj}H')}$$

$$h_7(j,n) = \frac{2Z_1(j,n)}{k_{oj}J_o^2(k_{oj})} \left[\sinh(k_{oj}L') - \cosh(k_{oj}L')h_6(j) \right]$$

$$Z_1(j,n) = \int_o^1 \eta J_o(k_{oj}\eta) \cos(\Delta_n \eta) \, d\eta$$

$$g_1(m) = \frac{-1}{\gamma_m I_1(\gamma_m)}$$

APPENDIX B

Kinetic Energy Integrals

The kinetic energy of a structural component of the system in three dimensional space is given by

$$T = \frac{\rho}{2} \iiint (\dot{u}^2 + \dot{v}^2 + \dot{w}^2)\, d(\text{Vol}).$$

This equation is written for each structural component of the system as follows:

$$T_t = \frac{\rho_t R^2 h_t}{2} \int_0^{L'} \int_0^{2\pi} (\dot{u}_t^2 + \dot{v}_t^2 + \dot{w}_t^2)\, d\theta\, d\xi$$

$$T_{tb} = \pi\, \rho_{tb}\, R^2 h_{tb} \int_{a'}^{1} \dot{u}_{tb}^2\, \eta\, d\eta$$

$$T_p = \pi\, \rho_p a^2\, h_p \int_0^{\ell'} (\dot{u}_p^2 + \dot{w}_p^2)\, d\epsilon$$

$$T_{pb} = \frac{1}{2}\, \pi\, \rho_{pb}\, a^2\, h_{pb}\, \dot{u}_{pb}^2$$

The kinetic energy of the liquid in the system is given by

$$T_\ell = \frac{\rho_\ell}{2} \iiint \nabla\phi \cdot \nabla\phi\; d(\text{Vol}).$$

Using Green's theorem (ref. 24), this can be simplified to

$$T_\ell = \frac{\rho_\ell}{2} \iint \phi\, \frac{\partial\phi}{\partial\eta}\, dS$$

The kinetic energy of the ullage gas is

$$T_g = \frac{1}{2}\, \pi\, \rho_{go} R^3 \int_0^{L'-H'} \dot{u}_g^2\, d\xi$$

Potential Energy Integrals

The strain energy in a cylindrical shell is given by the equation (ref. 25)

$$V = \frac{E}{2(1-\mu)} \iiint \left[\varepsilon_z^2 + \varepsilon_\theta^2 + 2\mu\varepsilon_z\varepsilon_\theta + \frac{1}{2}(1-\mu)\gamma_{z\theta}^2 \right] d(\text{Vol})$$

where

$$\varepsilon_z = \frac{\partial u}{\partial z} - (r-R)\frac{\partial^2 w}{\partial z^2}$$

$$\varepsilon_\theta = \frac{w}{R} + \frac{1}{R}\frac{\partial v}{\partial \theta} - \frac{r-R}{R^2}\frac{\partial^2 w}{\partial \theta^2}$$

$$\gamma_{z\theta} = \frac{1}{R}\frac{\partial u}{\partial \theta} + \frac{\partial v}{\partial z} - \frac{2(r-R)}{R}\frac{\partial^2 w}{\partial z \partial \theta} \quad .$$

The partial derivatives $\frac{\partial v}{\partial \theta}$ and $\frac{\partial v}{\partial z}$ have been considered negligible in the equation for ε_θ and $\gamma_{z\theta}$ above.

This equation is written in terms of the nondimensional co-ordinates for the tank and pipe.

$$V_t = \frac{K_t}{2}\int_0^{L'}\int_0^{2\pi} \left\{ \left(\frac{\partial u_t}{\partial \xi}\right)^2 + w_t^2 + \left(\frac{\partial v_t}{\partial \theta}\right)^2 + 2w_t\frac{\partial v_t}{\partial \theta} + 2\mu w_t \frac{\partial u_t}{\partial \xi} + 2\mu\frac{\partial u_t}{\partial \xi}\frac{\partial v_t}{\partial \theta} \right.$$

$$\left. + \frac{1}{2}(1-\mu)\left(\frac{\partial v_t}{\partial \xi}\right)^2 \right\} d\theta\, d\xi + \frac{D_t}{2R^2}\int_0^{L'}\int_0^{2\pi}\left\{ \left(\frac{\partial^2 w_t}{\partial \xi^2}\right)^2 + \left(\frac{\partial^2 w_t}{\partial \theta^2}\right)^2 \right.$$

$$\left. + 2\mu\frac{\partial^2 w_t}{\partial \xi^2}\frac{\partial^2 w_t}{\partial \theta^2} + 2(1-\mu)\left(\frac{\partial^2 w_t}{\partial \xi \partial \theta}\right)^2 \right\} d\theta\, d\xi$$

$$V_p = \pi K_p \int_0^{\ell'} \left\{ \left(\frac{\partial u_p}{\partial \varepsilon}\right)^2 + w_p^2 + 2\mu w_p\frac{\partial u_p}{\partial \varepsilon} \right\} d\varepsilon$$

$$+ \frac{\pi D_p}{a^2}\int_0^{\ell'}\left(\frac{\partial^2 w_p}{\partial \varepsilon^2}\right)^2 d\varepsilon$$

The equation for the strain energy of a circular plate in bending (ref. 26) is used to find the potential of the tank bottom in terms of the nondimensional coordinates.

$$V_{tb} = \frac{\pi D_{tb}}{R^2} \int_{a'}^{1} \left\{ \left(\frac{d^2 u_{tb}}{d\eta^2}\right)^2 - \frac{1}{2}(1-\mu)\frac{1}{\eta} \frac{du_{tb}}{d\eta} \frac{d^2 u_{tb}}{d\eta^2} + (1-\frac{\mu}{2}) \left(\frac{1}{\eta} \frac{du_{tb}}{d\eta}\right)^2 \right\} \eta \, d\eta$$

The potential energy of the gas is (ref. 19)

$$V_g = \frac{B}{2} \iiint \delta^2 \, d(Vol)$$

The dilatation (δ) is given by

$$\delta = \frac{1}{R} \frac{\partial u_g}{\partial \xi}$$

and the adiabatic bulk modulus (B) is related to the speed of sound by (ref. 27).

$$B = \rho_{go} c_o^2$$

This gives

$$V_g = \frac{1}{2} \pi R \rho_{go} c_o^2 \int_{0}^{L'-H'} \left(\frac{\partial u_g}{\partial \xi}\right)^2 \, d\xi.$$

APPENDIX C

Computer Program Details

GENERALIZED COORDS:
TANK U_1 PIPE U_1
TANK W_1 PIPE W_1
TANK U_2 PIPE U_2
TANK W_2 PIPE U_3
TANK U_3
TANK W_3

TANK:
LENGTH=120."
RADIUS=15."
THICKNESS=.016"
E=1X10^{7}PSI
BTM. THK.=.500"

PIPE:
LENGTH=90."
RADIUS=1.5"
THICKNESS=.022"
E=1X10^{7}PSI
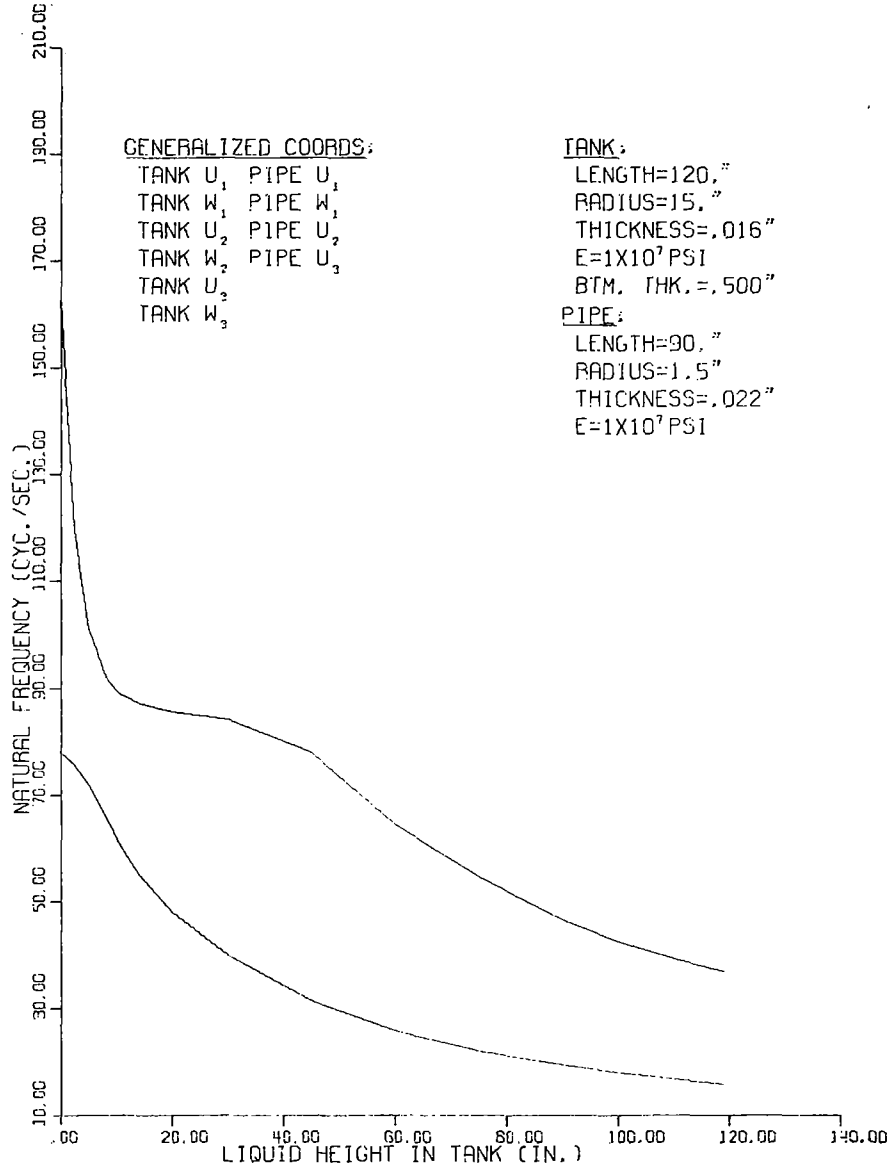
Figure C1.
Computer Plot for the Standard Configuration
with a Rigid Bottom and No Ullage Gas

37

START

READ TABLES
CJP, Z1

(89)

READ SWITCHES
NS1, NS2, NS3, NS4
FOR EXTENDED
OUTPUT

READ
CONFIGURATION
DATA

(1)

READ
GENERALIZED
COORDS.
NEED (I)

(87)

IS
EOF
Off   On

STOP

READ
H, IP, ICT

IS
IP=0? Yes

No

SET SOME
GENERALIZED
COORDS.
TO ZERO

PRINT
MESSAGE
FOR
ABOVE
ACTION

IS
CASE   Yes
NO.=1

No

PRINT CONFIG.
DATA
GENERALIZED
COORDS.
ETC.

COMPUTE VARIABLES
THAT WILL
REMAIN UNCHANGED
UNTIL IP CHANGES
VALUE

CONSIDER GENERALIZED COORDS.
TO DETERMINE BRANCHING CONTROLS
FOR INDIVIDUAL MATRIX ENTRIES.

UPPER TRIANGULAR FORM.

SET MATRIX
T(I,J) = 0
SET INDICATOR
IND = 0

(7777)

WITH IND=0, THE
MASS MATRIX IS
COMPUTED
WITH IND=1, THE
STIFFNESS MATRIX
IS COMPUTED

BRANCH ON JJ,J
VALUES TO COMPUTE
MATRIX ENTRIES

IS
EXTENDED
OUTPUT
SW. ON?   Yes

No

PRINT MATRIX
ENTRY, AND
ROW AND
COLUMN
NOS.

IS
IND-1
Neg.   Pos
Zero

4

T(I,J) = -T(I,J)

IS
EXTENDED
OUTPUT
SW. ON?   Yes

No

PRINT THE
MATRIX
T(I,J)

A(L,LL) = T(L,LL)
A IS THE
MASS
MATRIX
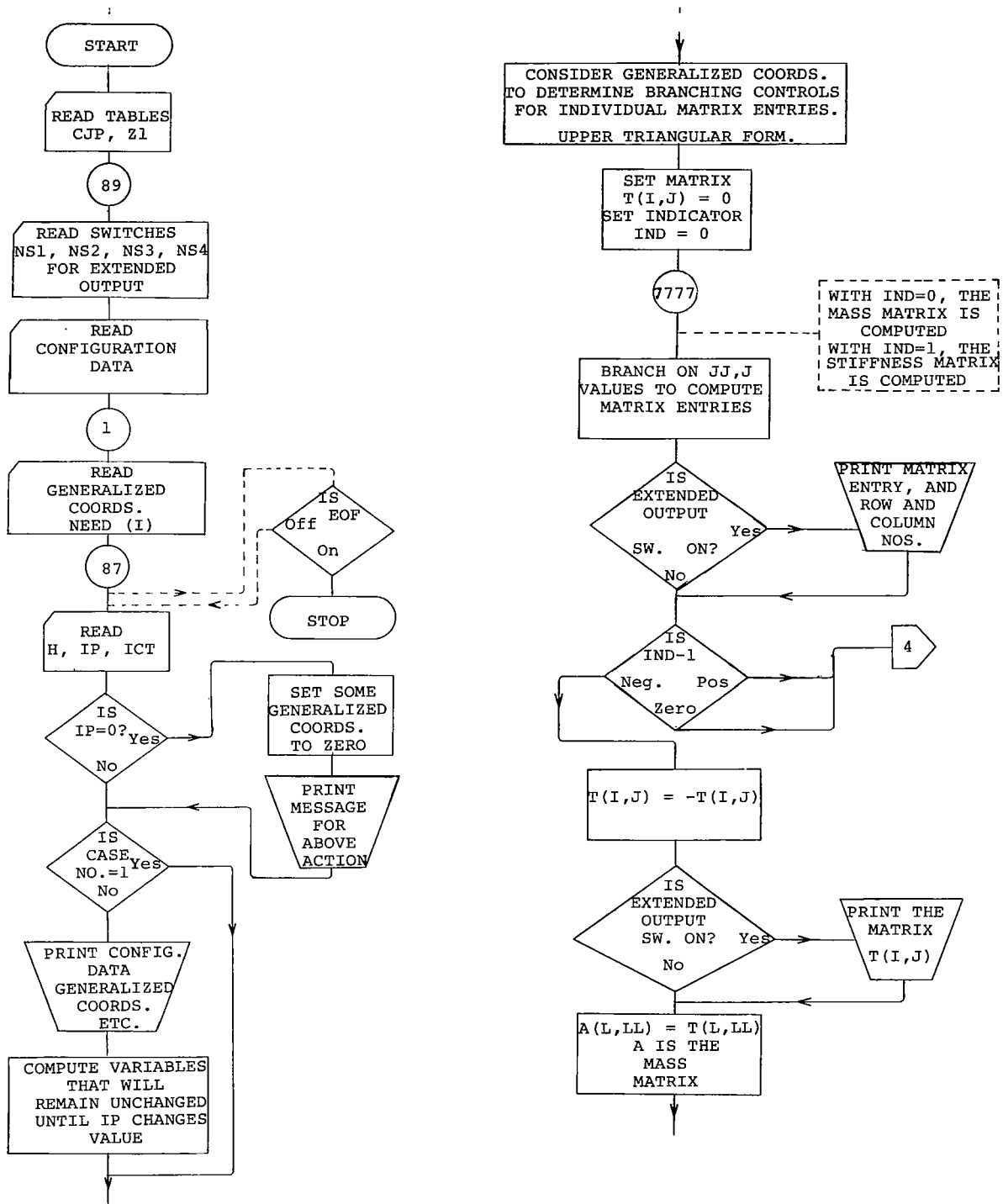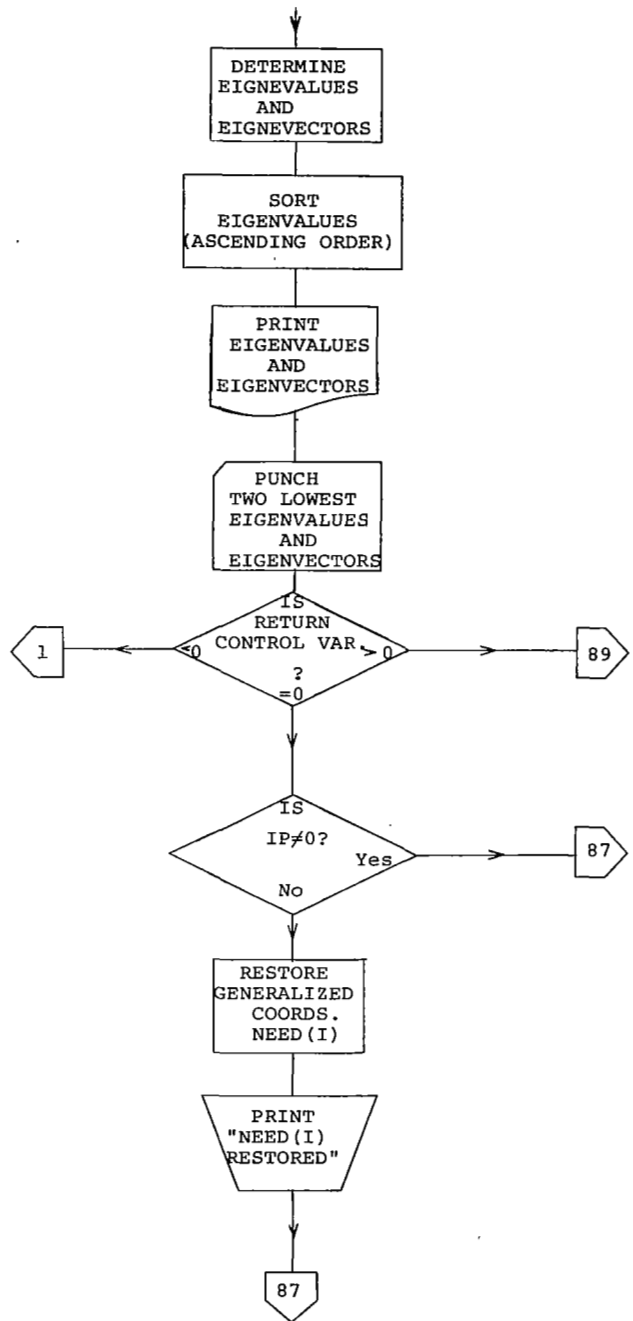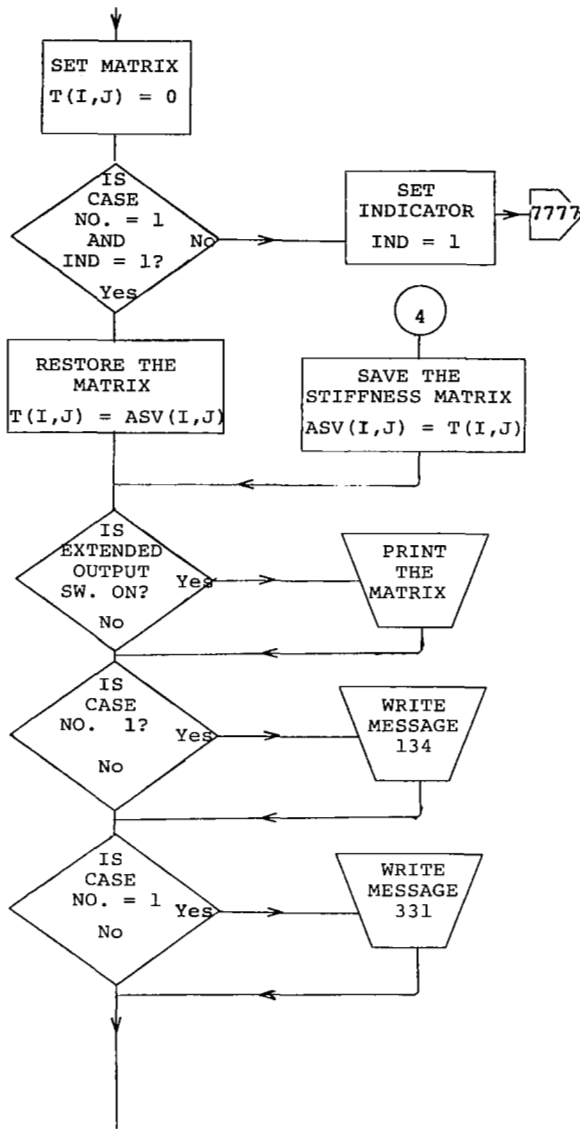
Figure C2.
Computer Program Flow Chart

Figure C2. (Continued)

**** TANK DIMENSIONS ****

LENGTH = 120.000 INCHES   RADIUS = 15.000 INCHES   THICKNESS = 0.0160 INCHES   BOTTOM THICKNESS = 0.5000 INCHES
DENSITY(MATERIAL)=0.25879988E-03 SLUGS/CU. INCH   MODULUS OF ELASTICITY=0.10000000E 08 PSI

** PIPE DIMENSIONS **

LENGTH = 90.000 INCHES   RADIUS = 1.500 INCHES   THICKNESS = 0.0220 INCHES   BOTTOM THICKNESS = 0.5000 INCHES
DENSITY(MATERIAL)+0.25879988E-03 SLUGS/CU. INCH   MODULUS OF ELASTICITY=0.10000000E 08 PSI

GRAVITATIONAL ATTRACTION= 386.40INCHES/SEC./SEC.   MU= 0.300   LIQUID DENSITY=0.93449999F-04 SLUGS/CU. INCH

GENERALIZED DISPLACEMENT COORDINATES CONSIDERED
                                        TANK   U SUB 1
                                        TANK   W SUB 1
                                        PIPE   U SUB 1
                                        PIPE   W SUB 1
                                        TANK   U SUB 2
                                        TANK   W SUB 2
                                        PIPE   U SUB 2
                                        TANK   U SUB 3
                                        TANK   W SUB 3
                                        PIPE   U SUB 3

THE 10 X 10 MATRIX, IN UPPER TRIANGULAR FORM, IS SOLVED

USING THE CONFIGURATION GIVEN ABOVE, WITH LIQUID HEIGHT= 0.0 INCHES, AND THE NO. OF CIRCUMFERENTIAL HALF-WAVES= 0   CASE 1

```
0.78188995E 02      4
0.16267899E 03      1
0.21850551E 03      7
0.91160986E 03      5
0.12764651E 04      3
0.17055801E 04      8
0.21869939E 04      2
0.22064351E 04      6
0.23209241E 04      9
0.32245195E 04     10
0.33398092E 00 -0.19660514E-01  0.10000000E 01  0.34489986E-01 -0.37466418E-01  0.17038848E-03 -0.78027427E-01  0.12196630E-01
-0.49217418E-02  0.44278163E-01
0.75100017E 00 -0.43704368E-01  0.10000000E 01 -0.47904916E-01 -0.75167060E-01 -0.13847763E-02 -0.13178980E 00  0.23873504E-01
-0.10840345E-01  0.14444473E-01
-0.34273183E 00  0.19691329E-01  0.10000000E 01 -0.14402218E-01  0.29843684E-01  0.15026771E-02 -0.11980408E 00 -0.91797300E-02
0.48402995E-02  0.19224305E-01
           .
           .
           .
```

NEED(I) RESTORED

ENCOUNTERED P=0,THUS SET NEED(I),I=5,6,12,13,19,20,26,27,33,34,40,41,47,48 ALL TO ZERO.

SAME CONFIGURATION AS ABOVE, EXCEPT WITH LIQUID HEIGHT= 5.00 INCHES, AND THE NO. OF CIRCUMFERENTIAL HALF-WAVES= 0   CASE 2

```
0.72050613E 02      4
0.10095039E 03      1
0.19149612E 03      7
           .
           .
           .
```

Figure C3.
Sample Computer Program Printout

LIST OF REFERENCES

1. Bauer, H.F.: Fluid Oscillations in a Circular Cylindrical Tank Due to Bending of the Tank Wall. Rept. No. DA-TR-3-58, ABMA, Redstone Arsenal, April, 1958.

2. Bauer, H.F.: Fluid Oscillations in the Containers of a Space Vehicle and Their Influence Upon Stability. NASA TR R-187, February, 1964.

3. Bauer, H.F.: The Response of Propellant in an Arbitrary Circular Cylindrical Tank Due to Single Pulse Excitation. Developments in Theoretical and Applied Mechanics, Proceedings of the Second Southeastern Conf., Atlanta, Ga., March 5-6, 1964, pp. 351-383.

4. Hutton, R.E.: An Investigation of Nonlinear, Nonplanar Oscillations of Fluid in a Cylindrical Container. Fifth AIAA Annual Structures and Materials Conf., Palm Springs, Calif., April 1-3, 1964.

5. Bhuta, P.G.; and Koval, L.R.: Hydroelastic Solution of the Sloshing of a Liquid in a Cylindrical Tank. J. Acoustical Soc. of America, vol. 36, no. 11, November, 1964, pp. 2071-2079.

6. Tong, P.: Liquid Motion in a Circular Cylindrical Container with a Flexible Bottom. AIAA Fifth Aerospace Sciences Mtg., Paper No. 67-76, New York, N.Y., January, 1967.

7. Fung, Y.C.; Sechler, E.E.; and Kaplan, A.: On the Vibration of Thin Cylindrical Shells under Internal Pressure. J. Aerospace Sci., vol. 24, no. 9, September, 1957, pp. 650-660.

8. Mixson, J.S.; and Herr, R.W.: An Investigation of the Vibration Characteristics of Pressurized Thin-Walled Circular Cylinders Partly Filled with Liquid. NASA TR R-145, 1962.

9. Leroy, J.: Vibrations de Respiration D'un Cylindre Mince Partiellement Rempli de Liquide. NASA Scientific and Technical Information Facility, N66-26732, 1965.

10. Chu, W.H.: A Theoretical Study of Nonlinear Fuel Sloshing in an Elastic Circular Tank. NASA CR-62151, Southwest Research Inst., San Antonio, Texas, 1964.

11. Chu, W.H.; and Kana, D.D.: A Theory for Nonlinear Transverse Vibrations of a Partially Filled Elastic Tank. NASA Contract No. NASr - 94(03), Southwest Research Inst., San Antonio, Texas.

12. Uchiyama, S.; and Tai, C.L.: A Study of Longitudinal Oscillations of Propellant Tanks and Wave Propagations in Feed Lines, Part V - Longitudinal Oscillations of a Propellant Filled Flexible Oblate Spheroidal Tank. NASA CR-74854, North American Aviation, Inc., Downey, Calif., March, 1966.

13. Runyan, H.L.; Pratt, K.G.; and Pierce, H.B.: Some Hydro-Elastic-Pneumatic Problems Arising in the Structural Dynamics of Launch Vehicles. National Conf. of the Aviation and Space Div. of the ASME, Los Angeles, Calif., March, 1965.

14. Pinson, L.D.; Leonard, H.W.; and Raney, J.P.: Analyses of the Longitudinal Dynamics of Launch Vehicles with Application to a 1/10-Scale Saturn V Model. AIAA J. Spacecraft and Rockets, vol. 5, no. 3, March 1968, pp. 303-308.

15. Pengelley, C.D.: Natural Frequency of Longitudinal Modes of Liquid Propellant Space Launch Vehicles. AIAA J. Spacecraft and Rockets, vol. 5, no. 12, December, 1968, pp. 1425-1431.

16. Streeter, V.L.: Fluid Dynamics. McGraw-Hill Book Company, Inc., New York, p. 26.

17. Lamb, H.: Hydrodynamics. Sixth Edition, Dover Publications, Inc., New York, 1945, pp. 363-364.

18. Goldstein, H.: Classical Mechanics. Addison-Wesley Publishing Company, Inc., Reading, Mass., 1950, p. 357.

19. Randall, R.H.: An Introduction to Acoustics. Addison-Wesley Press, Inc., Cambridge, Mass., 1951, Chpts. 2,6.

20. Rutherford, D.E.: Classical Mechanics. Second Edition, Interscience Publishers, Inc., New York, 1957, p. 170.

21. Hildebrand, F.B.: Methods of Applied Mathematics. Second Edition, Prentice-Hall, Inc., Englewood Cliffs, N.J., 1965, p. 69.

22. Howe, R.G.: The Calculation of Eigenvalues and Eigenvectors of ZV = LAV, wherein Z Is Real and Symmetric, V Is a Vector, L Is a Scalar, and A Is Real Symmetric Positive Definite. 1620 USERS Group, Computation Center, University of New Hampshire, Durham, New Hampshire, May, 1962.

23. Runyan, H.L.; Pratt, K.G.; and Pierce, H.B.; ibid.; p. 7.

24. Hildebrand, F.B., Advanced Calculus for Applications, Prentice-Hall, Inc., Englewood Cliffs, N.J., 1962, p. 293.

25. Hoff, N.J., The Analysis of Structures, John Wiley and Sons, Inc., New York, 1956, p. 131.

26. Den Hartog, J.P., Advanced Strength of Materials, McGraw-Hill Book Company, Inc., New York, 1952, p. 246.

27. Wood, A., Acoustics, Blackie and Son Limited, London & Glascow, 1940, p. 56.